J. Fluid Mech. (1984), *vol.* 145, *pp.* 275–285
Printed in Great Britain

Resonance in flows with vortex sheets and edges

By PAUL A. DURBIN
NASA Lewis Research Center, Cleveland, Ohio 44135

(Received 13 September 1983 and in revised form 5 April 1984)

It is shown that the vortex sheet in a slot between two semi-infinite plates does not admit incompressible resonant perturbations. The semi-infinite vortex sheet entering a duct does admit incompressible resonance. These results indicate that the vortex-sheet approximation is less useful for impinging shear flows than for non-impinging flows. They also suggest an important role of downstream vortical disturbances in resonant flows.

The general solution for perturbations to flow with a vortex sheet and edges is written in terms of a Cauchy integral. Requirements on the behaviour of this solution at edges and at downstream infinity fix the criteria for resonance.

1. Introduction

The phenomenon of self-sustained oscillation of an impinging shear flow has been known since the last century (see Rockwell & Naudascher 1979). However, a convincing fluid-mechanical analysis of this phenomenon has not yet been made; undoubtedly this is because of the subtlety of the interactions that lead to resonance. As a step toward producing such a fluid-mechanical analysis, Crighton & Innes (1981) recommended the study of idealized flow configurations in which the shear flow is replaced by a vortex sheet and surfaces are replaced by infinitely thin plates. The present paper follows that approach, and is further restricted to strictly *incompressible* flow: many experimentally observed resonances seem essentially to be incompressible, although without exact solutions for these flows an element of doubt remains. The purpose of this paper is to present one such exact solution.

The usual explanation of resonance in impinging shear flows (such as that sketched in figure 1, or that illustrated in figures 2.25 and 2.26 of Goldstein 1976) is that shear-flow instabilities originating at the upstream trailing edge grow into vortices, which impinge on the downstream leading edge and produce pressure oscillations which feed back to the upstream edge, regenerating the instability waves. The condition for resonance to occur is that the phase and amplitude changes around one cycle of this process be such that the original disturbance at the trailing edge is exactly regenerated by feedback.

This explanation is imprecise because it is not obvious what one should call the 'phase and amplitude changes' in a fluid flow. Analytically, it is more appropriate to associate resonance with eigensolutions to perturbation equations of motion. The above explanation also does not consider the fluid-mechanical processes that generate the feedback pressure at the downstream edge and which regenerate the instability waves at the upstream edge. In the present paper, where vortex sheets replace the shear flow, these interactions at edges are represented through edge conditions: the upstream condition is the Kutta condition of flow tangency; the downstream condition requires some special consideration. It is now well established that the Kutta

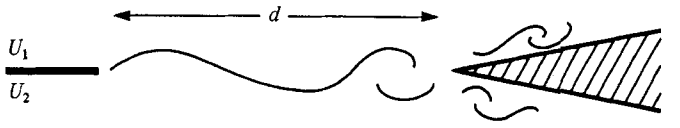

FIGURE 1. Mixing-layer–wedge flow.

condition correctly represents the flow past a trailing edge in the limit of infinite Reynolds number and finite frequency (Crighton 1981).

A method for analysing certain flows with vortex sheets and flat plates was presented by Möhring (1975). His method makes use of the analytic properties of the complex velocity potential, and at one stage certain arbitrary analytic functions are introduced into the analysis. These functions are subsequently determined by specifying edge singularities and the asymptotic behaviour at infinity. In §2 we give a method of analysis which is more direct than Möhring's and which is applicable to the same class of problems. This class of problems has a geometry that is symmetric about the vortex sheet. The approach used herein can be adapted to asymmetrical geometries, although closed-form solutions cannot then be found.

The present method is used to study two flows, one of which possesses resonant solutions and one of which does not. The flow without resonance is the slot flow, illustrated in figure 2. This flow was analysed by Möhring, who (despite certain errors in his solution) concluded that it does not admit resonance. Citing Möhring's errors, Crighton & Innes (1981) reanalysed the same slot problem, claiming that no solution existed unless a jump in the vortex-sheet displacement is introduced at the downstream edge. However, in discussing Möhring's analysis on p. 3 of their paper, Crighton & Innes erroneously required certain complex coefficients to be entirely real; apparently they failed to distinguish between Möhring's imaginary numbers i and j. The analysis we give in §3 shows that a jump in the vortex-sheet displacement at the downstream edge introduces a fictitious source into the flow. Therefore Crighton & Innes' analysis is of a vortex sheet *forced* by an oscillating source, not of self-excited resonant oscillations. Hence their conclusion that this flow possesses resonant solutions is a misinterpretation. Similarly Howe's (1981*a*) solution of this problem, which is singular at the downstream edge, ought to be considered a forced solution, not a resonant one. However, Howe's paper dealt mainly with acoustic disturbances to vortex sheets, and he also observed that no resonance could occur if the downstream singularity were removed. This agrees with the conclusion reached previously by Möhring.

Presumably resonance can occur in mixing-layer–wedge experiments (figure 1) because the mixing layer has a finite width and does not terminate at the downstream edge as idealized in figure 2. Vortical disturbances then can continue to evolve in the shear flow downstream of the leading edge (Goldstein 1981; Ziada & Rockwell 1981); *these vortical disturbances seem to be an essential part of the downstream resonant flow.* Of course the experimental flow usually contains finite-amplitude vortices, while the vortex-sheet analysis is linear, but we suspect that this is not the source discrepancy.

After concluding in §3 that the slot problem is too idealized to describe resonance in an impinging shear flow, a flow with a non-impinging vortex sheet is analysed in §4. Our method of solution requires that the geometry be symmetric across the vortex sheet, so the flow of a vortex sheet into a duct is considered (figure 3). In this flow the vortex sheet extends beyond the leading edge, so downstream vortical disturbances exist. Presumably this is one reason why this flow does admit resonant solutions.

It also seems necessary, in order to satisfy resonance criteria on 'amplitude and phase', that there be (at least) two free non-dimensional parameters in the problem. In the slot problem (figure 2) the only parameter is the Strouhal number based on slot width, while in the duct-entry problem (figure 3) there is an additional length ratio. (Another way of viewing the role of finite shear-layer width in the mixing-layer–wedge flow is that it provides a second parameter.) However, the existence of two parameters is probably not sufficient for resonance to occur: in calculations not reported here we were unable to find resonance when the slot flow was enclosed in an infinite duct. Admittedly, the final step in this analysis consisted of a *numerical* search for zeros of a complex-valued function, so the failure to find resonance might be considered inconclusive.

The duct-entry problem (figure 3) was discussed by Möhring (1975). The solution that he described is inappropriate because it grows as $e^{\frac{1}{2}n\pi x}$, with n an odd integer, as $x \to \infty$ inside the duct. This solution does not oscillate spatially and its growth is independent of its temporal frequency. Möhring incorrectly refers to it as a 'Kelvin–Helmholtz instability'; it is better described as an 'edge singularity' associated with an 'edge' at infinity. Thus Möhring's solution omits the spatially growing Kelvin–Helmholtz wave. That is why he concluded erroneously that this problem has no incompressible resonant solutions.

Analysis of the flow in figure 3 is complicated by the exponentially unbounded growth down the duct of the vortex-sheet oscillations. For this reason, the analysis in §4 starts with a solution for the flow depicted in figure 4, having a plate inside the duct. Then the plate is moved to downstream infinity. In this way, a family of resonant solutions is found.

2. Method of solution

Consider a two-dimensional time-dependent disturbance to a horizontal mean flow containing a vortex sheet and horizontal flat plates. Away from the sheet and plates, the disturbance is irrotational and its complex velocity $w(z) = u - iv$ is an analytic function of $z = x + iy$. On the solid plates $v = 0$, while across the vortex sheet the pressure and the vertical displacement of fluid particles must be continuous. These continuity conditions are most easily satisfied if the complex particle displacement $\chi(z) = \xi - i\eta$ is introduced. Here $(\xi(x, y), \eta(x, y))$ is the displacement by the perturbation of the particle at (x, y) from its initial position. (The convenience of working with the dependent variable χ was pointed out to me by Dr M. E. Goldstein.) The connection between χ and w is $w = \mathrm{D}\chi/\mathrm{D}t$, where as usual $\mathrm{D}/\mathrm{D}t = \partial/\partial t + U\partial/\partial x$ for a uniform flow U in the x-direction. Under the assumption of small perturbations to a uniform flow, the momentum equation can be written as

$$\frac{\mathrm{D}^2\chi}{\mathrm{D}t^2} = -\frac{\partial p}{\partial x} + i\frac{\partial p}{\partial y}. \tag{1}$$

If [ ] denotes the jump across the vortex sheet of the bracketed quantity, then continuity of pressure across a vortex sheet lying along $y = 0$ requires $[\partial p/\partial x] = 0$ or, by (1),

$$\left[\frac{\mathrm{D}^2\xi}{\mathrm{D}t^2}\right] = 0. \tag{2}$$

We will require that the flow geometry be symmetric with respect to reflection across the line $y = 0$ containing the vortex sheet. This allows χ to be written in terms of

FIGURE 2. Slot problem.

functions symmetric and antisymmetric in y. The condition of mass continuity requires that $[\eta] = 0$, so η must be symmetric, The corresponding ξ is antisymmetric, as is seen from the Cauchy–Riemann relations. Consequently $\xi_1 = -\xi_2 = \frac{1}{2}\Delta\xi$, where ξ_1 (ξ_2) is the limit of ξ as the vortex sheet is approached from above (below). The mean velocity is U_1 (U_2) above (below) $y = 0$. Of course $\Delta\xi = [\xi]$. Equation (2) now reduces to

$$\frac{\mathrm{D}_1^2\Delta\xi}{\mathrm{D}t^2} + \frac{\mathrm{D}_2^2\Delta\xi}{\mathrm{D}t^2} = 0, \tag{3}$$

where

$$\frac{\mathrm{D}_i}{\mathrm{D}t} = \frac{\partial}{\partial t} + U_i\frac{\partial}{\partial x} \quad (i = 1, 2).$$

If $\Delta\xi$ has an $\mathrm{e}^{\mathrm{j}\omega t}$ time dependence, the solution to (3) is

$$\Delta\xi = \mathrm{e}^{\mathrm{j}\omega t}\{A\,\mathrm{e}^{\epsilon_+ x} + B\,\mathrm{e}^{\epsilon_- x}\}, \tag{4a}$$

where A and B are arbitrary constants (which are real with respect to i) and

$$\epsilon_\pm = \frac{-\mathrm{j} \pm \lambda}{\frac{1}{2}(1+\lambda^2)(U_1+U_2)}, \tag{4b}$$

with

$$\lambda = \frac{U_1 - U_2}{U_1 + U_2} > 0. \tag{4c}$$

In the following the factor $\mathrm{e}^{\mathrm{j}\omega t}$ will be suppressed. The two terms in (4a) are growing and decaying instability waves. In (4) j denotes $\sqrt{-1}$, as does i in (1). Two different letters are used because their i-dependence determines the analytic properties of functions of z, whereas their j-dependence reflects the behaviour with time; in analytical considerations j should be treated as real. This distinction between i and j is made to avoid confusion; it will not figure importantly in the following.

Equation (3) follows from pressure continuity and $\Delta\eta = [\eta] = 0$ follows from mass continuity. Furthermore, on any horizontal surface the condition of flow tangency is that $\eta = 0$. Because χ is an analytic function away from the vortex sheet and boundaries, it is determined by $\Delta\xi$, $\Delta\eta$, the boundary condition $\eta = 0$, and its asymptotic behaviour at ∞.

For the problems presently being considered, a conformal mapping of the $z(= x + \mathrm{i}y)$-plane to the $\tau(= \zeta + \mathrm{i}\sigma)$-plane exists which maps the vortex sheet and all boundaries onto the line $\sigma = 0$. The vortex sheet may be taken to lie on $-c \leqslant \zeta \leqslant c$ provided that there are plates which extend to upstream and downstream ∞. The τ-plane is depicted in figure 2. It is essential that the geometry in the z-plane (e.g. figures 3 and 4) is symmetric about the vortex sheet, for then opposing points above and below the sheet are mapped into opposing points; in other words, $\Delta\xi(x) = \Delta\xi(\zeta)$ when ζ is the image of x.

It now follows from the Plemlj formulas (Roos 1969, p. 231) that

$$\chi(\tau) = \xi - \mathrm{i}\eta = \frac{1}{2\pi\mathrm{i}(c^2-\tau^2)^{\frac{1}{2}}}\left[\int_{-c}^{c} \frac{(c^2-\tau^2)^{\frac{1}{2}}}{t-\tau}\Delta\xi(t)\,\mathrm{d}t + C\tau + D\right], \tag{5}$$

where C and D are real constants (real with respect to i), is a solution satisfying the jump and boundary conditions, and is bounded as $\tau \to \infty$. When the z-domain is unbounded it is appropriate to require that χ tend to zero as $\tau \to \infty$; then $C = 0$. When the flow is enclosed in an infinite duct in the z-plane $C \neq 0$. Branch cuts for the square roots in (5) lie along $\sigma = 0$, $|\zeta| > c$. Thus $\eta = 0$ along the solid boundaries $\sigma = 0$, $|\zeta| > c$ because the right-hand side of (5) is real there, and $[\eta] = 0$ because the real part of the integral in (5) is continuous across the vortex sheet. The imaginary part of the integral suffers a jump of $2\pi i(c^2 - \tau^2)^{\frac{1}{2}} \Delta\xi(z)$ so that the jump condition on ξ is met. Furthermore, (5) is the *unique* analytic function satisfying the jump and boundary conditions, and having no worse than a square-root singularity at $\zeta = \pm c$ (Roos 1969).

The solution (5) has been obtained for a symmetric geometry. For an asymmetric geometry conformal transformations can be applied separately to the upper and lower half-planes. In the upper plane η is given by an expression like (5), but with ξ_1 appearing under the integral; in the lower plane η is given by a similar expression with ξ_2 under the integral. Equating these expressions for η gives an integral equation which must be solved along with (2) for ξ_1 and ξ_2. This poses a difficult mathematical problem.

Equations (5) and (4a) determine the oscillatory flow which accompanies a Kelvin–Helmholtz wave on the vortex sheet. They contain four unspecified constants: A, B, C and D. From here on we consider only the case $C = 0$. Since homogeneous boundary conditions have been specified, (5) is an eigensolution. The amplitude of this eigensolution is arbitrary, and for this reason so is one of A, B or D. The other constants, and the criterion for resonance, must be determined by imposing edge conditions.

Referring to figure 2, because the vortex sheet leaves the upstream edge (5) must be made to satisfy $\eta(-c) = 0$ on $\sigma = 0$. Furthermore, in order that the perturbation velocity be finite at the trailing edge, the Kutta condition (Crighton 1981) $\partial\eta(-c)/\partial\zeta = 0$ must be imposed. It follows from (5) that these conditions require

$$\int_{-c}^{c} \left(\frac{c-t}{c+t}\right)^{\frac{1}{2}} \Delta\xi(t)\,\mathrm{d}t + D = 0, \tag{6a}$$

$$\int_{-c}^{c} \frac{1}{(c+t)^{\frac{1}{2}}} \frac{\mathrm{d}}{\mathrm{d}t}((c-t)^{\frac{1}{2}} \Delta\xi(t))\,\mathrm{d}t = 0. \tag{6b}$$

Equation (6a) follows immediately from (5); (6b) requires some manipulation before it can be written as a convergent integral. Note that by (4a) the left-hand sides of (6) are complex in the variable j, so both real and imaginary parts must vanish. Together, (6a) and (6b) determine two of the complex (with respect to j) coefficients A, B and D.

We have now constructed an eigensolution, valid for all ω, which satisfies appropriate trailing-edge conditions; however, nothing has been required of the downstream behaviour of this solution. In general, the downstream behaviour is *not arbitrary*. At least one further constraint of the type (6) must be imposed. This last constraint overspecifies the solution; or alternatively it makes it so that solutions can exist only for certain frequencies, if they exist at all. But because the constraints are complex-valued a second parameter, say d, in addition to frequency, is generally required to satisfy the downstream constraint. d is a parameter associated with the flow geometry (see figure 3). Thus one expects solutions only for certain values of ω and d. Such solutions are eigensolutions satisfying physically appropriate constraints,

and the pair (ω, d) is the eigenvalue. These solutions could be imagined to arise spontaneously in the flow; they are the self-sustained oscillations presently being sought.

3. Vortex sheet in a slot

Previous analyses of the flow depicted in figure 2 were discussed in §1. The solution given by Möhring (1975) contains incorrectly evaluated integrals, but when these are evaluated properly it appears to be correct. His method for deducing this solution is quite different from that used here. For that reason it is hoped that the present reworking of this problem will not be considered redundant.

For the present problem the z- and τ-planes described in §2 are the same. Thus (4a) can be substituted directly into (5) to find

$$\chi = \frac{1}{2\pi \mathrm{i}(c^2-\tau^2)^{\frac{1}{2}}}\left[\int_{-c}^{c} \frac{(c^2-t^2)^{\frac{1}{2}}}{t-\tau}(A\,\mathrm{e}^{\epsilon+t}+B\mathrm{e}^{\epsilon-t})\,\mathrm{d}t+D\right], \tag{7}$$

and similarly for the edge conditions (6). It remains to specify the behaviour of χ at the downstream edge, $\tau = c$.

Suppose $\eta(x)$ were known on the vortex sheet. Then since $\eta(x) = 0$ for $|x| > c$ on $y = 0$, the complex velocity that vanished as $|\tau| \to \infty$ would be

$$u - \mathrm{i}v = -\frac{1}{\pi}\int_{-c}^{c} \frac{\mathrm{D}_1\eta}{\mathrm{D}t}(x)\frac{\mathrm{d}x}{x-\tau} \tag{8a}$$

in the upper half-plane and

$$u - \mathrm{i}v = \frac{1}{\pi}\int_{-c}^{c} \frac{\mathrm{D}_2\eta}{\mathrm{D}t}(x)\frac{\mathrm{d}x}{x-\tau} \tag{8b}$$

in the lower half-plane. This follows from Cauchy's formula (Roos 1969). Upon letting $|\tau| \to \infty$, substituting the definition of $\mathrm{D}/\mathrm{D}t$, and noting that $\eta(-c) = 0$, one finds that

$$u - \mathrm{i}v \to \begin{cases} \dfrac{1}{\pi\tau}\left[U_1\,\eta(c) + \displaystyle\int_{-c}^{c} \frac{\partial\eta}{\partial t}(x)\,\mathrm{d}x\right] & \text{in the upper plane,} \\ -\dfrac{1}{\pi\tau}\left[U_2\,\eta(c) + \displaystyle\int_{-c}^{c} \frac{\partial\eta}{\partial t}(x)\,\mathrm{d}x\right] & \text{in the lower plane.} \end{cases} \tag{9}$$

It follows that the net mass flux through a large circle about the origin is $(U_1 - U_2)\,\eta(c)$. So in the absence of oscillating sources in the flow we must have $\eta(c) = 0$. Thus Crighton & Innes' (1981) suggestion that $\eta(c)$ be non-zero appears to correspond to the introduction of a mass source. This conclusion drawn from (9) is based on the present requirement that $\eta = 0$ on the downstream plate. Howe (1981b) allowed η to be non-zero on $x > c$, regarding this as a model of downstream Tolmein–Schlichting waves. The above argument does not apply to Howe's model, because the excess mass flux is compensated there by boundary-layer oscillations.

The condition $\eta(c) = 0$ implies

$$\int_{-c}^{c} \left(\frac{c+t}{c-t}\right)^{\frac{1}{2}}(A\,\mathrm{e}^{\epsilon+t}+B\,\mathrm{e}^{\epsilon-t})\,\mathrm{d}t - D = 0 \tag{10}$$

by (7). Collecting (6*a*, *b*) and (10) and evaluating the integrals gives

$$\left.\begin{aligned} A[I_0(w_+)-I_1(w_+)]+B[I_0(w_-)-I_1(w_-)]+D/c &= 0,\\ A[2w_+(I_0(w_+)-I_1(w_+))-I_0(w_+)]+B[2w_-(I_0(w_-)-I_1(w_-))-I_0(w_-)] &= 0,\\ A[I_0(w_+)+I_1(w_+)]+B[I_0(w_-)+I_1(w_-)]-D/c &= 0, \end{aligned}\right\} \quad (11)$$

where $w_\pm = c\epsilon_\pm$ and I_0, I_1 are modified Bessel functions. These equations have a non-trivial solution only if

$$2(w_+-w_-)\,I_0(w_+)\,I_0(w_-) = w_+\,I_0(w_-)\,I_1(w_+)-w_-\,I_0(w_+)\,I_1(w_-). \quad (12)$$

Because $w_- = -w_+^*$, the left-hand side of this is real and the right-hand side is imaginary. Thus both sides must vanish, which is clearly impossible as the left-hand side equals $4\,\mathrm{Re}\,(w_+)|I_0(w_+)|^2 \neq 0$. Thus we conclude that *there are no solutions to the slot problem satisfying the appropriate edge conditions.*

As was mentioned in §1, an analysis of the slot flow enclosed in an infinite duct also failed to yield resonant solutions. It appears that the condition $\eta(c) = 0$ prevents resonance; the evolution of the shear flow downstream of the impingement edge seems to be the feature missing from these slot flows. Howe's (1981*b*) model of boundary oscillations is one method for rectifying this situation. However, there is an *ad hoc* element to this type of model, which for the present we wish to avoid. Instead we examine the flow depicted in figure 3, which has a non-impinging semi-infinite shear layer. Although this flow may seem a bit contrived, nevertheless it could conceivably be the infinite-Reynolds-number limit of a realizable shear flow. The main purpose of the present paper is to show that incompressible resonance can occur in such a flow.

4. Vortex sheet entering a duct

Recognizing also that at least two non-dimensional parameters seem required to satisfy resonance criteria, the duct-entry flow of figure 3 seems a promising source of resonant solutions. A difficulty that arises in finding solutions for this flow can be seen immediately from (5): $\Delta\xi$ becomes exponentially unbounded as $x\to\infty$, so the integration over the vortex sheet may diverge. A device for avoiding this divergence is to add a downstream plate inside the duct (figure 4) and then find the asymptotic solution for this flow as the leading edge of the plate tends to ∞; the result should be a solution for the flow of figure 3, except in a neighbourhood of the 'plate at infinity'. (It is remarked in §1 that Möhring's exponentially growing solution is really a singularity at the edge of this plate at infinity.)

In order to apply the method of §2, a conformal mapping from the z-plane of figure 4 to the τ-plane of figure 2 is required. The inverse of this mapping is

$$z = \tau-a-1-\ln(\tau-a)+\pi\mathrm{i}, \quad (13)$$

where the branch cut of the logarithm is along $\sigma = 0$, $\zeta > a$; recall that $\tau = \zeta+\mathrm{i}\sigma$. The normalization in (13) is such that the duct height is 2π. Referring to figures 2 and 4, one finds the relations

$$d = c+a+1+\ln(c+a), \qquad l = c-a-1-\ln(a-c) \quad (14)$$

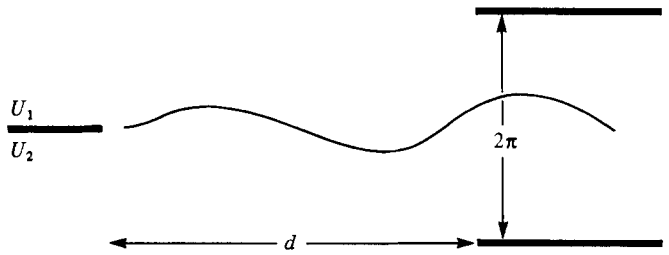

FIGURE 3. Duct-entry problem.

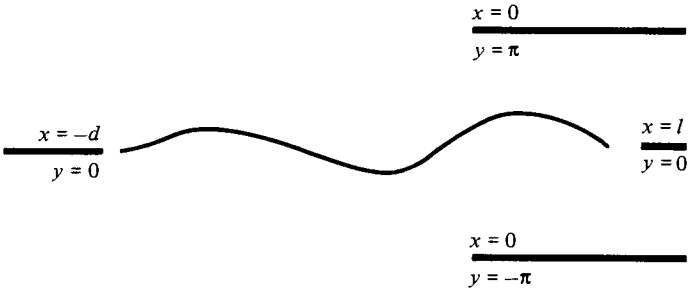

FIGURE 4. Duct-entry with downstream plate.

between a, c, and d, l. The point $\tau = a$ is the image of $x = \infty$ inside the duct. Thus, as the edge inside the duct tends to infinity, $c \to a$. Then (14) becomes

$$d \approx 2c + 1 + \ln 2c, \qquad a \approx c + \mathrm{e}^{-l-1}. \tag{15}$$

Using (13) to substitute ζ for x in (4a), and substituting the result into (5), gives

$$\chi = \frac{1}{2\pi\mathrm{i}(c^2-\tau^2)^{\frac{1}{2}}}\left[\int_{-c}^{c} \frac{(c^2-t^2)^{\frac{1}{2}}}{t-\tau}\left(\frac{A\,\mathrm{e}^{\epsilon+t}}{(a-t)^{\epsilon+}} + \frac{B\,\mathrm{e}^{\epsilon-t}}{(a-t)^{\epsilon-}}\right)\mathrm{d}t + D\right], \tag{16}$$

where constants have been absorbed into A and B. The edge conditions (6) can be rewritten similarly. It remains to impose a downstream constraint on the solution, and to find the asymptotic behaviour when $a \to c$.

It can be shown, essentially by the method used in Durbin (1979), that, as $\tau \to c$ and $a \to c$, χ can be expanded into two series of the form

$$\chi = (c-\tau)^{-\epsilon+}(O(1) + O(c-\tau) + O(c-\tau)^2 \ldots), \\ + (c-\tau)^{-\frac{1}{2}}(O(1) + O(c-\tau) + O(c-\tau)^2 \ldots) \tag{17}$$

(plus terms $O(c-\tau)^{-\epsilon-}$). The explicit forms of the $O(1)$ terms are given in

$$\chi = (c-\tau)^{-\epsilon+}\left[\frac{A\,\mathrm{e}^{c\epsilon+}}{(1+[a-c]/[c-\tau])^{\epsilon+}} + \frac{A\,\mathrm{e}^{c\epsilon+}}{2\pi\mathrm{i}} \oint_0^{\infty} \frac{x^{\frac{1}{2}}}{(1-x)\,(x+[a-c]/[c-\tau])^{\epsilon+}}\mathrm{d}x + \ldots\right] \\ + \frac{(c-\tau)^{-\frac{1}{2}}}{2(2c)^{\frac{1}{2}}\pi\mathrm{i}}\left[D - B\int_{-c}^{c} \frac{(c+x)^{\frac{1}{2}}}{(c-x)^{\epsilon-+\frac{1}{2}}}\mathrm{e}^{\epsilon-x}\,\mathrm{d}x - A\oint_{-c}^{c} \frac{(c+x)^{\frac{1}{2}}}{(c-x)^{\epsilon++\frac{1}{2}}}\mathrm{e}^{\epsilon+x}\,\mathrm{d}x + \ldots\right], \tag{18}$$

where $\int$ is a principal value and $\oint$ is the generalized interpretation of a divergent integral (Lighthill 1975). The expansion (18) breaks down when $|c-\tau| \ll a-c = \mathrm{e}^{-l-1}$, i.e. in a small neighbourhood of the 'edge at infinity'. This edge was introduced as an artifice in our solution procedure, so the solution in its vicinity is not of interest.

The first term in (18) is the Kelvin–Helmholtz wave, which, using (13) to substitute for $c-\tau$, grows like $e^{\epsilon_+ x}$ as $x\to\infty$. The second term in (18) is an edge singularity, which grows like $e^{\frac{1}{2}x}$; clearly such growth is unphysical and must be eliminated. Thus our downstream condition is that the coefficient of $(c-\tau)^{-\frac{1}{2}}$ in (18) vanishes:

$$D-B\int_{-c}^{c}\frac{(c+x)^{\frac{1}{2}}}{(c-x)^{\epsilon_- +\frac{1}{2}}}e^{\epsilon_- x}\,dx-A\int_{-c}^{c}\frac{(c+x)^{\frac{1}{2}}}{(c-x)^{\epsilon_+ +\frac{1}{2}}}e^{\epsilon_+ x}\,dx=0. \tag{19}$$

Note that this condition is analogous to (10).

The complex coefficients, say A and B, and real parameters c and ω, of our problem are now determined by the three complex equations (6a, b) and (19). On letting $a\to c$ in (6) one finds that the integrals diverge if $\mathrm{Re}\,(\epsilon_+)\geqslant\frac{3}{2}$. In what follows it will be required that

$$\mathrm{Re}\,(\epsilon_+)<\tfrac{3}{2}, \tag{20}$$

or, by use of (4b), that

$$\frac{\tilde{\omega}\lambda}{\frac{1}{2}(1+\lambda^2)}<\tfrac{3}{2}.$$

Here $\tilde{\omega}$ is the non-dimensional frequency

$$\tilde{\omega}=\frac{\omega H}{2\pi(U_1+U_2)},$$

where H is the duct height.

It is not necessary that condition (20) be imposed. When (20) is not satisfied it is appropriate to interpret the divergent integrals in (6) and in (22) in a generalized sense. Or, alternatively, the integrals involving ϵ_+ can be evaluated by analytic continuation in the complex ϵ-plane.

Condition (6) and (19) can be combined, and when (20) is satisfied they give the relation that determines $\tilde{\omega}$ and c:

$$J(\epsilon_+)\,L(\epsilon_-)-J(\epsilon_-)\,L(\epsilon_+)=0, \tag{21}$$

with

$$\left.\begin{aligned} J(\epsilon)&=\frac{e^w}{2^{\epsilon-1}}+\int_{-1}^{1}\frac{e^{wt}(1+2w(t-1-1/c)-e^w(1-2\epsilon)\,[\frac{1}{2}(1+t)]^{\frac{1}{2}}}{(1-t)^{\epsilon}\,(1-t^2)^{\frac{1}{2}}}\,dt,\\ L(\epsilon)&=\int_{-1}^{1}\frac{e^{wt}}{(1-t)^{\epsilon-\frac{1}{2}}(1+t)^{\frac{1}{2}}}\left[1+\frac{w(1+t)+\frac{1}{2}}{\frac{1}{2}-\epsilon}\right]dt, \end{aligned}\right\} \tag{22}$$

$w=c\epsilon$. The integrals in (22) have been manipulated to put them into forms that converge under (20). Equation (21) is the eigenvalue relation defining the resonance condition.

Roots of (21) were found numerically. Library subroutines were used to evaluate integrals by the Romberg method and to find roots by the secant method. The secant routing required fairly good initial guesses: these were obtained by printing out tables of the modulus of the left-hand-side of (21) and searching through them for minima. Starting from these, the roots $\tilde{\omega}$ and c were found. d was obtained from c by (15).

Figures 5 and 6 show the roots $\tilde{\omega}$ and d as functions of λ. At given λ these figures show a set of frequencies and distances at which resonance occurs. The limit $\tilde{\omega}(\lambda)$ defined by (20) is also shown in figure 5. Our numerical algorithm failed when roots approached this curve, so it was not possible to determine how this limit is approached. The curves shown in figure 5 simply terminate where we stopped tracing them numerically. Often this was where the numerical algorithm began to fail; either

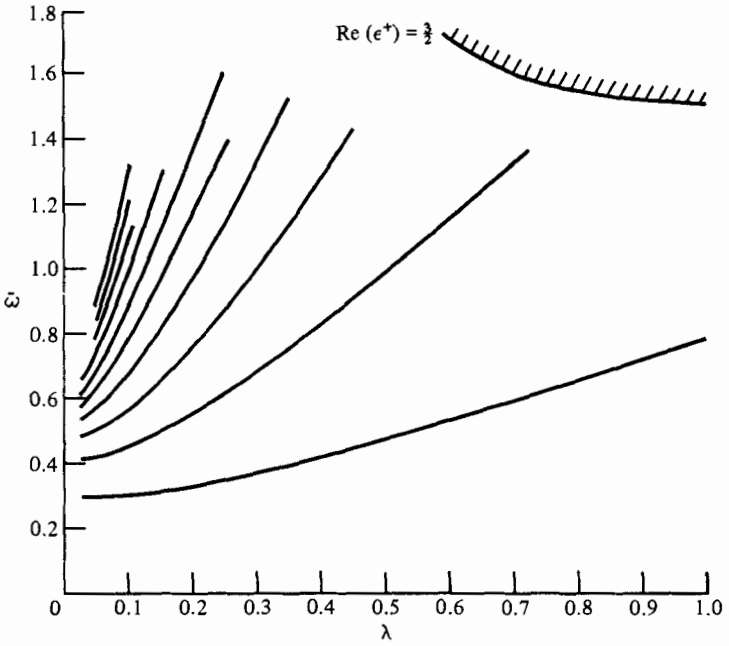

FIGURE 5. Resonant frequencies versus velocity difference.

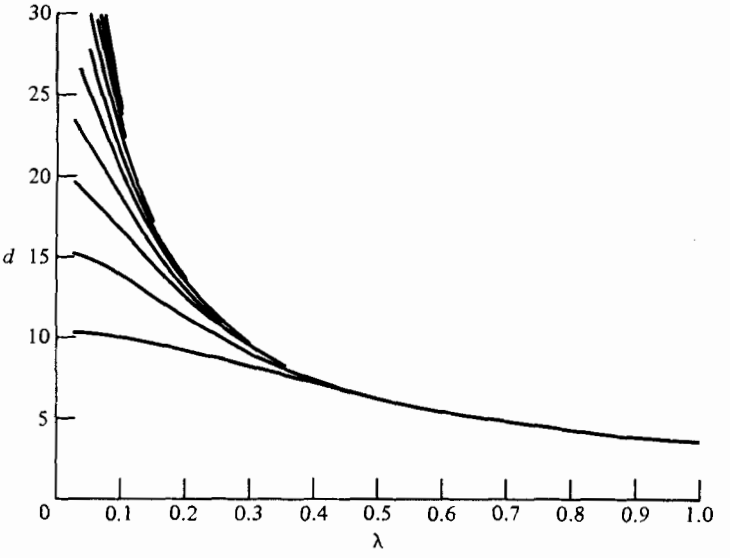

FIGURE 6. Resonant distances versus velocity difference.

because the curve where integrals diverge was approached, or because the oscillations of the integrand decreased numerical accuracy. Presumably, the curves shown in figure 5 extend to all values of λ and constitute an infinite set of resonant frequencies.

Figure 6 shows the distances of the plate from the duct at which resonance occurs. These curves appear to coalesce as λ is increased. However, our numerical results do not permit us to say absolutely that the curves converge without crossing.

The solution that has been derived for the duct-entry problem provides an instance of resonance in incompressible flow. In order to obtain a simple exact solution it was

necessary to consider a highly idealized flow. Because the downstream vortex sheet is bounded by walls on both sides, the duct-entry flow is quite different from the impinging mixing layer (figure 1). Also, the mixing layer has finite width, while the vortex sheet is infinitely thin. For these reasons little comparison can be made between the present results and existing experiments. In order to study experimentally the flow of figure 3 one would have to ensure that the duct height and instability wavelength were large compared with the shear-layer thickness.

I am grateful to Dr M. E. Goldstein for discussing this analysis with me.

REFERENCES

CRIGHTON, D. G. 1981 Acoustics as a branch of fluid mechanics. *J. Fluid Mech.* **106**, 261–298.

CRIGHTON, D. G. & INNES, D. 1981 Analytical models for shear-layer feedback cycles. *AIAA Paper* 81–0061, presented at the 19th Aerospace Sciences Meeting, St. Louis, MO.

DURBIN, P. A. 1979 Asymptotic expansion of Laplace transforms about the origin using generalized functions. *J. IMA* **23**, 181–192.

GOLDSTEIN, M. E. 1976 *Aeroacoustics*. McGraw-Hill.

GOLDSTEIN, M. E. 1981 The coupling between flow instabilities and incident disturbances at a leading edge. *J. Fluid Mech.* **104**, 217–246.

HOWE, M. S. 1981*a* The influence of mean shear on unsteady aperture flow, with application to acoustical diffraction and self-sustained cavity oscillations. *J. Fluid Mech.* **109**, 125–146.

HOWE, M. S. 1981*b* On the theory of unsteady shearing flow over a slot. *Phil. Trans. R. Soc. Lond.* A **303**, 151–180.

LIGHTHILL, M. J. 1975 *Introduction to Fourier Analysis and Generalized Functions*. Cambridge University Press.

MÖHRING, W. 1975 On flows with vortex sheets and solid plates. *J. Sound Vib.* **38**, 403–412.

ROCKWELL, D. & NAUDASCHER, E. 1979 Self-sustained oscillations of impinging free shear layers. *Ann. Rev. Fluid Mech.* **11**, 67–94.

ROOS, B. W. 1969 *Analytic Functions and Distributions in Physics and Engineering*. Wiley.

ZIADA, S. & ROCKWELL, D. 1982 Oscillations of an unstable mixing layer impinging upon an edge. *J. Fluid Mech.* **124**, 307–334.